J|A|C|S
ARTICLES
Published on Web 02/01/2003

# DNA−Dye Conjugates for Controllable H* Aggregation[1]

Hiroyuki Asanuma,*[,†,‡] Kenji Shirasuka,[†] Tohru Takarada,[†,§] Hiromu Kashida,[†] and Makoto Komiyama*[,†]

*Contribution from the Research Center for Advanced Science and Technology, The University of Tokyo, Komaba, Meguro-ku, Tokyo 153-8904, Japan, and PRESTO, Japan Science and Technology Corporation (JST), Kawaguchi 332-0012, Japan*

Received September 5, 2002; E-mail: asanuma@mkomi.rcast.u-tokyo.ac.jp, komiyama@mkomi.rcast.u-tokyo.ac.jp

***Abstract:*** Methyl Red H* aggregate of predetermined size is successfully synthesized from the DNA conjugate involving multiple Methyl Red moieties in sequence. In the single stranded state, hypsochromicity monotonically increases with the number of incorporated dyes: the peak maximum of the conjugate involving six Methyl Reds appears at 415 nm, and the shift is as great as 69 nm (3435 $cm^{-1}$) with respect to the monomeric transition. This large hypsochromicity accompanied by the narrowing of the band clearly demonstrates that H* aggregate is formed in the single strand. H* aggregation is further promoted at higher ionic strength. Upon addition of complementary DNA below the $T_m$, however, this H* band disappears and a new peak appears at 448 nm, indicating that aggregated structure is changed by the duplex formation. This spectral change is completely reversible so that the H* band at 415 nm appears again above $T_m$. Thus, aggregated structure can be reversibly controlled by the formation and dissociation of the DNA duplex.

## Introduction

Aggregation of dye molecules is known to affect spectroscopic behaviors due to the coherent coupling of dye excitation. Depending on the aggregated structure and the number of aggregation (size), a large bathochromic (J-aggregate) or hypsochromic (H-aggregate) shift is induced (see Supporting Information Figure 1).[2] Since these dye aggregates have distinct optical properties that the corresponding monomeric dyes do not show, they have been widely investigated from scientific and practical points of view.[3] One of the important themes in this field is how to prepare a stable dye aggregate of predetermined size and how to regulate its aggregated structure reversibly.[4,5] Dye aggregates are conventionally prepared by the self-association of individual dye monomers in solution so that the size of aggregates is difficult to control. Moreover, higher aggregates always precipitate from the solution. Overgrowth of the aggregates can be restricted only when some kind of templates or supports for the dyes exist in the solution.[6] To our knowledge, simple vinyl polymer carrying dyes are not very successful for this purpose. Reversible regulation of the aggregated structure is still more difficult, because most of self-associated aggregates take only one thermodynamically stable structure.

Here, we apply phosphoramidite chemistry developed for DNA synthesis to the preparation of dye aggregates because (1) the number of aggregation and arrangement of dyes are easily controllable by programming the sequence, (2) sufficient solubility in water, where dye aggregation preferentially occurs, is provided by the anionic backbone of the phosphodiester linkage, and (3) reversible regulation of aggregated structure is possible on hybridization with complementary DNA. Recent advances in phosphoramidite chemistry have extended the kinds of monomers for DNA synthesis, so that various molecules are now available as a monomer.[7] Dye oligomers can be synthesized from phosphoramidite monomer carrying dye molecule and are easily incorporated into natural oligonucleotides by use of DNA synthesizer.

In the present paper, Methyl Red H* aggregate of predetermined size is successfully synthesized in the single strand by introducing multiple Methyl Red moieties into natural DNA.[8,9] By hybridization with complementary DNA, the H* aggregate

[†] The University of Tokyo.
[‡] JST.
[§] Current address: Department of Applied Chemistry, Graduate School of Engineering, Kyushu University, Hakozaki, Higashi-ku, Fukuoka 812-8581 Japan.

(1) A preliminary communication: Asanuma, H.; Shirasuka, K.; Komiyama, M. *Chem. Lett.* **2002**, 490−491.
(2) (a) McRae, E. G.; Kasha, M. *J. Chem. Phys.* **1958**, *28*, 721−722. (b) Norland, K.; Ames, A.; Taylor, T. *Photogr. Sci. Eng.* **1970**, *14*, 295−307. (c) Knapp, E. W. *Chem. Phys.* **1984**, *85*, 73−82.
(3) (a) Asanuma, H.; Tani, T. *J. Phys. Chem. B* **1997**, *101*, 2149−2153. (b) Daehne, L.; Kamiya, K.; Tanaka, J. *Bull. Chem. Soc. Jpn.* **1992**, *65*, 2328−2332. (c) Tani, T. *Photographic Sensitivity*; Oxford University Press: Oxford, U.K., 1995; p 111, and references therein.
(4) Note that both the size of aggregation and the aggregated structure affect the spectroscopic properties. See Supporting Information Figure 1.
(5) Place, I.; Perlstein, J.; Penner, T. L.; Whitten, D. G. *Langmuir* **2000**, *16*, 9042−9048.
(6) (a) Wang, M.; Silvia, G. L.; Armitage, B. A. *J. Am. Chem. Soc.* **2000**, *122*, 9977−9986. (b) Seifert, J. L.; Connor, R. E.; Kushon, S. A.; Wang, M.; Armitage, B. A. *J. Am. Chem. Soc.* **1999**, *121*, 2987−2995. (c) Hill, D. J.; Mio, M. J.; Prince, R. B.; Hughes, T. S.; Moore, J. S. *Chem. Rev.* **2001**, *101*, 3893−4011.
(7) (a) Kool, E. T. *Chem. Rev.* **1997**, *97*, 1473−1488. (b) Tanaka, K.; Shionoya, M. *J. Org. Chem.* **1999**, *64*, 5002−5003. (c) Meggers, E.; Holland, P. L.; Tolman, W. B.; Romesberg, F. E.; Schultz, P. G. *J. Am. Chem. Soc.* **2000**, *122*, 10714−10715. (d) Ogawa, A. K.; Wu, Y.; McMinn, D. L.; Liu, J.; Schultz, P. G.; Romesberg, F. E. *J. Am. Chem. Soc.* **2000**, *122*, 3274−3287, and references therein.
(8) H aggregate is a supramolecule which shows hypsochromic shift of the $\lambda_{max}$ with respect to the corresponding monomeric transition by the stacking of dyes along the vertical axis of the dye plane. See ref 2 and Supporting Information Figure 1.

***Scheme 1.*** Synthesis of Phosphoramidite Monomer Involving Methyl Red Moiety (A) and Modified DNAs Prepared in the Present Study (B)

(A)

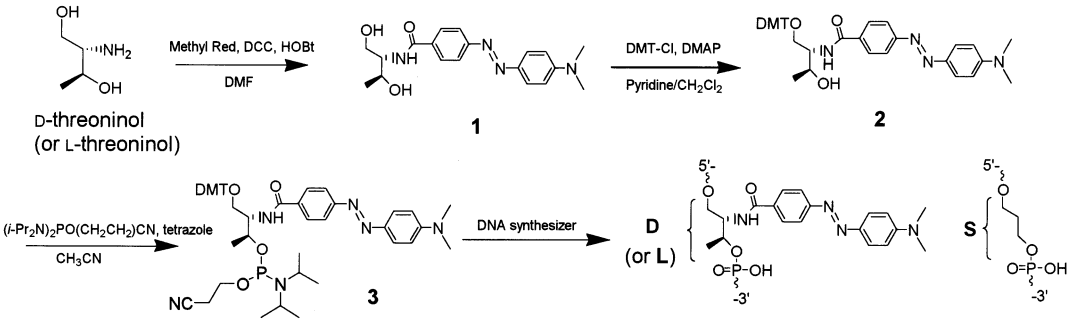


(B)

**D0**: 5'-GGT-ATC-GCA-ATC-3'
**D1**: 5'-GGT-ATC-**D**-GCA-ATC-3'
**D2**: 5'-GGT-ATC-**DD**-GCA-ATC-3'
**D3**: 5'-GGT-ATC-**DDD**-GCA-ATC-3'
**D4**: 5'-GGT-ATC-**DDD-D**-GCA-ATC-3'
**D5**: 5'-GGT-ATC-**DDD-DD**-GCA-ATC-3'
**D6**: 5'-GGT-ATC-**DDD-DDD**-GCA-ATC-3'

**L1**: 5'-GGT-ATC-**L**-GCA-ATC-3'
**L2**: 5'-GGT-ATC-**LL**-GCA-ATC-3'
**L6**: 5'-GGT-ATC-**LLL-LLL**-GCA-ATC-3'

**DS4**: 5'-GGT-ATC-**DSD-SDS-DS**-GCA-ATC-3'

**S0**: 3'-CCA-TAG-CGT-TAG-5'
**S1**: 3'-CCA-TAG-**S**-CGT-TAG-5'
**S2**: 3'-CCA-TAG-**SS**-CGT-TAG-5'
**S3**: 3'-CCA-TAG-**SSS**-CGT-TAG-5'
**S4**: 3'-CCA-TAG-**SSS-S**-CGT-TAG-5'
**S5**: 3'-CCA-TAG-**SSS-SS**-CGT-TAG-5'
**S6**: 3'-CCA-TAG-**SSS-SSS**-CGT-TAG-5'

**C1**: 3'-CCA-TAG-5' **C2**: 3'-CGT-TAG-5'

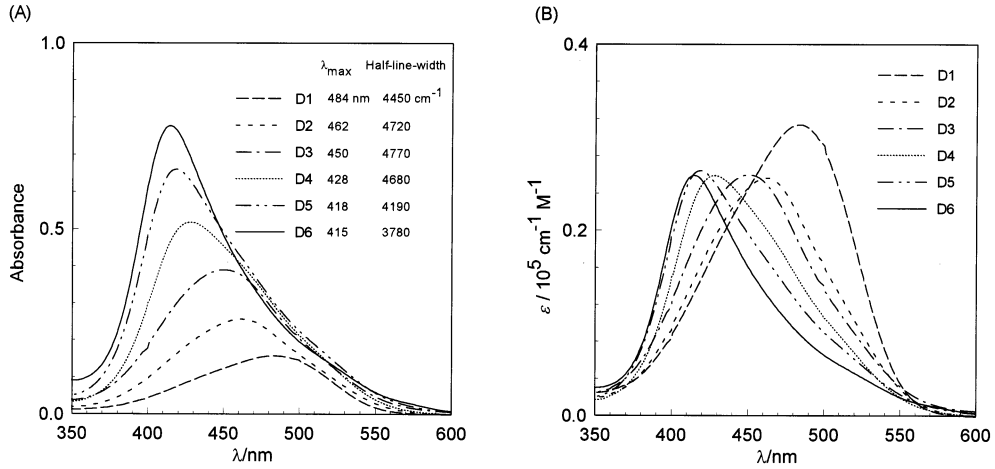


***Figure 1.*** UV−vis spectra of single stranded **D*n*** involving various numbers of Methyl Red moieties on D-threoninol. Absorbance of **D*n*** solution is shown in A, whereas the molar extinction coefficient of Methyl Red in each **D*n*** solution is shown in B. Spectroscopic measurements were carried out at 0 °C, pH 7.0 (10 mM phosphate buffer), in the presence of 0.1 M NaCl. The concentration of each **D*n*** is 5 $\mu$M.

is reversibly converted into a new dye aggregate of different structure, which can be controlled by the kinds of DNAs used for hybridization. Predominance of the DNA−Methyl Red conjugate as a controllable aggregate is demonstrated.

## Results

**H* Aggregation in Single Stranded DNA by the Sequential Introduction of Multiple Methyl Reds.** Introduction of Methyl Red moieties (**D** or **L** residues in Scheme 1) was carried out on a DNA synthesizer through the corresponding phosphoramidite monomer synthesized according to Scheme 1A. All the modified DNAs are also listed in Scheme 1B. Figure 1 shows absorption spectra of various DNA conjugates involving multiple Methyl Reds on D-threoninols. The half-line-width and $\lambda_{max}$ are also presented in the inset. A single stranded DNA involving one Methyl Red moiety (**D1**) shows monomeric transition whose $\lambda_{max}$ appears at 484 nm (the broken line in the bottom of Figure 1A).[10] Significantly, sequential introduction of multiple Methyl Reds in the DNA induces distinct hypsochromic shift. Hypsochromicity monotonically increases with the number of incorporated Methyl Reds. For instance, when three Methyl Reds are introduced (**D3** in Figure 1A), $\lambda_{max}$ appears at 450 nm whose hypsochromic shift with respect to **D1** is 34 nm. With a small

(9) In the case in which both hypsochromicity and narrowing of the band are induced, it is called H* aggregate (see Supporting Information Figure 1). Only limited examples of the H* aggregate have been reported so far: (a) Herz, A. H. *Photogr. Sci. Eng.* **1974**, *18*, 323. (b) Tanaka, J. In *Relaxation of Elementary Excitations*; Kubo, R., Hanamura, F., Eds.; Springer-Verlag: Berlin, 1980; p 181.

(10) Absorption spectrum of aqueous solution of Methyl Red shows $\lambda_{max}$ at 463 nm (Supporting Information Figure 2), which corresponds to the $\pi-\pi^*$ transition of Methyl Red in the monomeric state. The bathochromic shift of $\lambda_{max}$ (463−484 nm) by the introduction of Methyl Red into DNA could be interpreted as stacking with adjacent nucleobases.

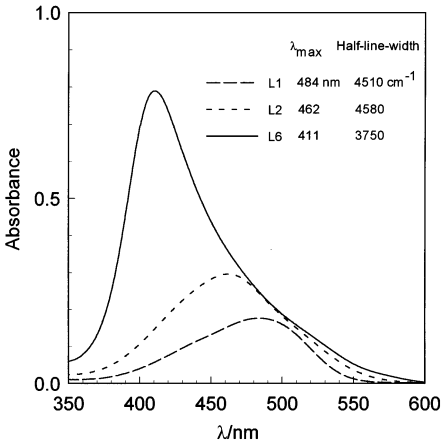


***Figure 2.*** UV−vis spectra of single stranded **L*n*** on L-threoninol involving various numbers of Methyl Red moieties at 0 °C, pH 7.0 (10 mM phosphate buffer), in the presence of 0.1 M NaCl. The concentration of each **L*n*** is 5 $\mu$M.

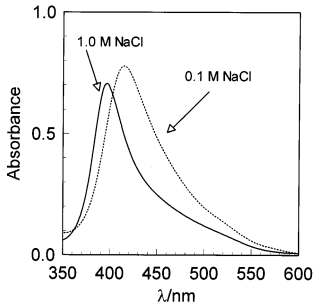


***Figure 3.*** Effect of ionic strength on the H* aggregation of **D6**. Spectroscopic measurements were carried out at 0 °C, pH 7.0 (10 mM phosphate buffer), in the presence of 0.1 M NaCl (dotted line) or 1.0 M NaCl (solid line).

number of dyes in the DNA such as **D2** and **D3**, broadening of the bands is observed.[11] On the contrary, further multiplication of Methyl Reds induces narrowing of the bands (see **D4** to **D6**). Especially for **D6**, the half-line-width is about 700 $cm^{-1}$ narrower than that of **D1**, and the absorption maximum appears at 415 nm, corresponding to a 69 nm (3435 $cm^{-1}$) hypsochromic shift with respect to **D1**. A similar hypsochromic shift is also observed by multiplication of Methyl Reds on L-threoninols (compare Figure 2 with Figure 1A). These results are consistent with the molecular exciton theory predicting that an increase in the number of aggregation accompanies a larger hypsochromic shift.[2a] The H* band of **D6** shows further hypsochromic shift (from 415 to 397 nm) and narrowing (from 3780 to 2850 $cm^{-1}$) by raising the concentration of NaCl from 0.1 to 1.0 M (see Figure 3). Thus, H* aggregates of predetermined sizes are prepared in the single stranded DNA.[9] It should be noted that all these H* aggregates are sufficiently stable in water and no precipitation occurs even at 0 °C at high salt concentration.

Together with this strong hypsochromicity, hypochromicity due to the stacking interaction is also observed. The molar extinction coefficient of Methyl Red at the peak maximum of **D6** is much smaller than that of **D1** (compare **D6** with **D1** in Figure 1B).[12] Similarly, higher H* aggregation at higher NaCl concentration also causes further hypochromicity of the band (Figure 3).

(11) Aggregates of Methyl Reds in **D2** and **D3** are not H* but H aggregates because they show only hypsochromicity without narrowing of the band. See refs 8 and 9.

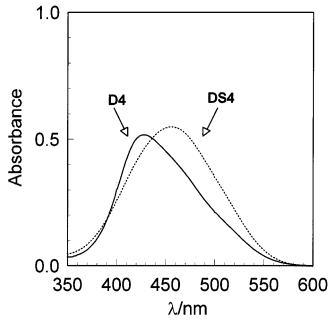


***Figure 4.*** UV−vis spectra of single stranded **D4** (solid line) and **DS4** (dotted line) at 0 °C, pH 7.0 (10 mM phosphate buffer), in the presence of 0.1 M NaCl. The concentration of each conjugate is 5 $\mu$M.

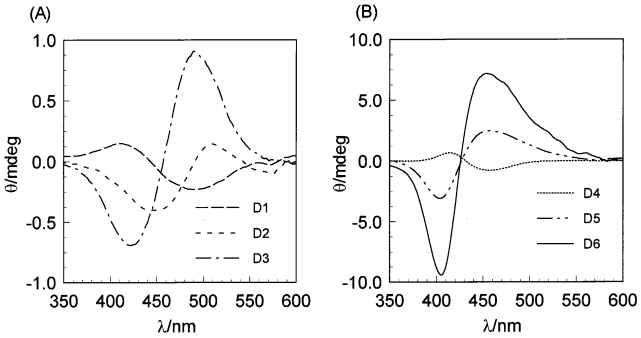


***Figure 5.*** CD spectra of single stranded **D1**−**D3** (A) and **D4**−**D6** (B). Spectroscopic measurements were carried out at 0 °C, pH 7.0 (10 mM phosphate buffer) in the presence of 0.1 M NaCl. The concentration of each **D*n*** is 5 $\mu$M. Note that the vertical axis in A is reduced to one-tenth with respect to that in B.

Sequential introduction of Methyl Reds in the DNA is essential for the aggregation. Thus, the H* aggregate is not formed when **D** and the 1,3-propanediol residue (**S**) are alternately incorporated: absorption maximum of **DS4** with four pairs of alternating **D** and **S** appears at 457 nm (dotted line in Figure 4), whereas the $\lambda_{max}$ of **D4** with four sequential **D** residues is 428 nm (solid line in Figure 4).

Since all the **D*n*** series synthesized here are chiral and optically pure, distinct circular dichroism (CD) is observed in the absorption spectrum of the dye (Figure 5A,B). These CD signals also reflect the strong exciton coupling due to the aggregation: as the number of **D** residue increases, the CD signal is drastically magnified because exciton coupling among identical chromophores (the origin of CD) is enhanced by multiplication of dyes.[13] Interestingly, most of the **D*n*** series ($n \geq 2$) show a positive Cotton effect, indicating that they take similar helical structure (vide infra).[14−16]

**Structural Change of H* Aggregate on Hybridization of DNA−Dye Conjugates with Their Complementary Strands.** The aggregated structure is controllable by hybridization. When **S6** is added, the H* band of **D6** at 415 nm disappears and a new peak appears at 448 nm (compare solid line with dotted

(12) Since the absorption band of **D6** becomes narrower than that of **D1**, the oscillator strength is weakened by H* aggregation.
(13) The CD signal of the dye absorption for **D1** arises from the interaction between the nearby base pairs and Methyl Red.
(14) Although **D4** shows the reversed-phase CD signal compared with other **D*n*** series at 0 °C, the temperature elevation above 20 °C induces the same phase CD (see Supporting Information Figure 3). Assumedly, H* aggregate of **D4** would be not so rigid and sensitive to the environment.
(15) Berova, K.; Nakanishi, K.; Woody, R. W. *Circular Dichroism; Principles and Applications*, 2nd ed.; VCH Publishers: New York, 2000.
(16) Rodger, A.; Nordén, B. *Circular Dichroism and Linear Dichroism*; Oxford University Press: Oxford, U.K., 1997; p 72.

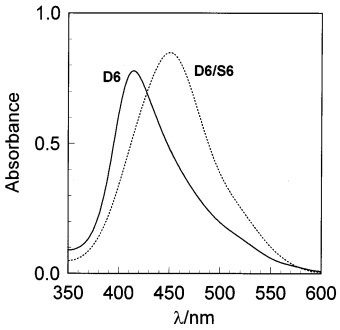


***Figure 6.*** UV−vis spectra of **D6** in the absence (solid line) and presence (dotted line) of **S6** at 0 °C, pH 7.0 (10 mM phosphate buffer) in the presence of 0.1 M NaCl.

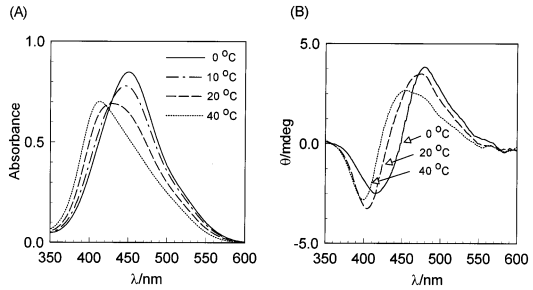


***Figure 7.*** Temperature dependence of UV−vis (A) and CD (B) spectra of **D6**/**S6** duplex at pH 7.0 (10 mM phosphate buffer) in the presence of 0.1 M NaCl. The concentrations of **D6** and **S6** are 5 and 6 $\mu$M, respectively.

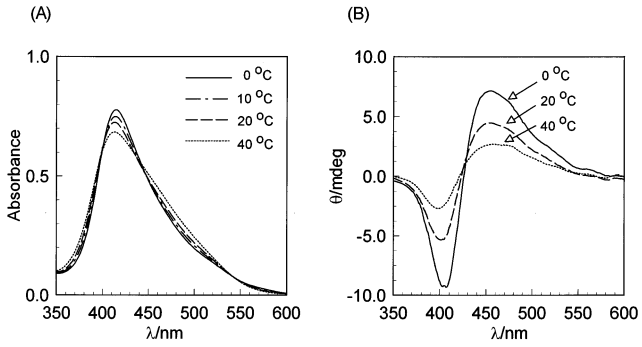


***Figure 8.*** UV−vis (A) and CD (B) spectra of single stranded **D6** at various temperatures at pH 7.0 (10 mM phosphate buffer) in the presence of 0.1 M NaCl. The concentration of **D6** is 5 $\mu$M.

line in Figure 6). On hybridization, the CD signal also shifts toward longer wavelength (see solid line in Figure 7B). These spectroscopic changes clearly demonstrate that a new aggregate of different structure is formed in the duplex. On elevating temperature above $T_m$ (21.1 °C as estimated from the melting curve at 260 nm under the conditions employed), the peak at 448 nm disappears and the H* band at 415 nm appears again due to the removal of **S6** from **D6** (dotted line in Figure 7A). This change of UV−vis spectrum is completely reversible so that the peak at 448 nm appears again below $T_m$. Similarly, the CD spectrum also reversibly changes by varying the temperature (see Figure 7B). Thus, the aggregated structure can be reversibly controlled by the formation and dissociation of the DNA duplex. Consistently, the absorption maximum of the UV−vis spectrum of **D6** in the absence of **S6**, as well as the shape and position of its induced CD, is almost independent of the temperature (Figure 8). Two different structures of the aggregates can be reversibly prepared from **D6** either by the hybridization of **S6** or by its dissociation.

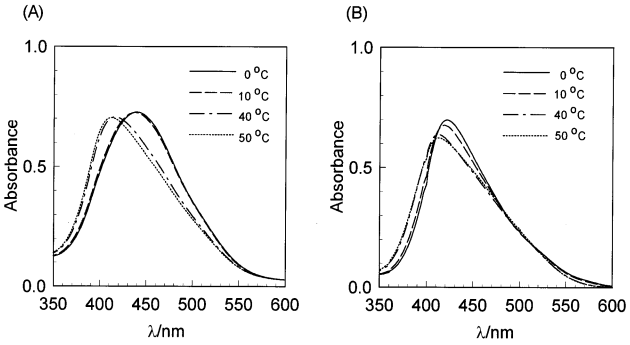


***Figure 9.*** UV−vis spectra of **D6**/**S0** duplex (A) and **D6**/**C1**/**C2** ternary system (B) at pH 7.0 (10 mM phosphate buffer) in the presence of 0.1 M NaCl at various temperatures. The $T_m$s of **D6**/**S0** and **D6**/**C1**/**C2** were 37.7 and 13.5 °C as estimated from the melting curve at 260 nm under the conditions employed.

To induce this structural change of the H* aggregate, the complementary DNA should involve both **C1** and **C2** sequences in the 3′ and 5′ sides, respectively. They must be covalently bound to each other. Consistently, natural DNA (**S0**), which has both **C1** and **C2** sequences but no **S** residues, also induces a large bathochromic shift on the hybridization with **D6** ($\lambda_{max}$ = 439 nm at 0 °C; see the solid line in Figure 9A), although the spectrum is different from that of the **D6**/**S6** duplex ($\lambda_{max}$ = 448 nm at 0 °C; see the solid line in Figure 7A). In contrast, the bathochromic shift is very small, when **D6** is separately hybridized with two natural DNAs **C1** and **C2** (Figure 9B).

**Effect of the Number of S Residues in the Complementary Strand on the Spectroscopic Behaviors of D5.** The results of the previous section demonstrate that hybridization of the DNA−Methyl Red conjugate with the complementary strand affects the structure of aggregated dyes. Here, spectroscopic behavior of **D5** on hybridization is investigated systematically by varying the number of **S** residues in the complementary strand. Since both **D5** and **S*n*** (***n*** ≥ 1) involve nonnatural residues, $T_m$s of the duplexes are lower than that of corresponding natural **D0**/**S0** duplex without **D** and **S** (48.0 °C as estimated from the melting curve at 260 nm under the conditions employed). The $T_m$s of **D5**/**S*n*** duplexes monotonically decrease as the number of **S** residues increases, as listed in Table 1.[17] Since the minimum $T_m$ is 27.2 °C (for **D5**/**S6** duplex), spectroscopic measurements are carried out at 0 °C where duplexes are firmly formed.

When **D5** is hybridized with **S0**, the sharp H* band of **D5** disappears and a new broad peak appears at 439 nm (dotted line in Figure 10A). The UV spectrum is similar to that of **D5**/**S1**. But, as the number of **S** residues increases, $\lambda_{max}$ of the **D5**/**S*n*** duplex monotonically shifts toward longer wavelength (see Figure 10A and Table 1). Together with this bathochromic shift, both distinct narrowing of the band and an increase in absorbance at $\lambda_{max}$ are simultaneously observed. Thus, the aggregated dye structure in the duplex is controllable by the number of the spacers in the complementary strand.

The number of **S** residues also affects the CD spectra (Figure 10B). On hybridization with **S0**, the CD signal of **D5** shifts toward longer wavelength and is weakened (dotted line in Figure

(17) The melting curves of **D5**/**S*n*** duplexes are depicted in Supporting Information Figure 4A. For reference, $T_m$ curves of **D*m*/S2** ($2 \le m \le 5$) are also included in Supporting Information Figure 4B.

***Table 1.*** Effect of the Number of the **S** Residues on Melting Temperature ($T_m$) and on Spectroscopic Behavior of **D5/S*n***[a]

| | | spectroscopic params[c] | | |
|---|---|---|---|---|
| strand(s) | $T_m$ [b]/°C | $\lambda_{max}$/nm | absorbance | half-line-width/cm$^{-1}$ |
| **D5** | | 418 | 0.66 | 4190 |
| **D5/S0** | 36.3 | 439 | 0.62 | 5140 |
| **D5/S1** | 35.8 | 440 | 0.62 | 5160 |
| **D5/S2** | 32.9 | 443 | 0.64 | 4870 |
| **D5/S3** | 31.2 | 448 | 0.67 | 4550 |
| **D5/S4** | 30.0 | 451 | 0.72 | 4250 |
| **D5/S5** | 27.6 | 452 | 0.74 | 4130 |
| **D5/S6** | 27.2 | 453 | 0.74 | 4200 |

[a] Spectroscopic measurement was carried out at 0 °C, pH 7.0 (10 mM phosphate buffer), in the presence of 0.1 M NaCl. The concentrations of **D5** and **S*n*** were 5 and 6 $\mu$M, respectively. [b] $T_m$ was determined from the change of absorbance at 260 nm as a function of temperature (See Experimental Section for the detail). The melting curves of **D5/S*n*** are also presented in Supporting Information Figure 4A. The $T_m$ of natural **D0/S0** duplex without **D** or **S** residue was 48.0 °C. [c] Absorbance and half-line-width were obtained from the absorption band at $\lambda_{max}$.

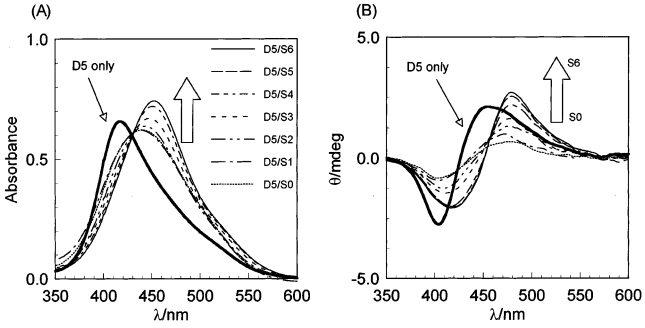


***Figure 10.*** UV−vis (A) and CD (B) spectra of **D5/S*n*** duplexes at 0 °C, pH 7.0 (10 mM phosphate buffer), in the presence of 0.1 M NaCl.

10B). The weakened CD is again intensified by the increase in the number of **S** residues, as observed in the UV spectra.[18]

## Discussion

**H* Aggregation by Multiplication of Methyl Reds in Single Stranded DNA.** Sequential multiplication of Methyl Reds induces a large hypsochromic shift and narrowing of the band. Thus, H* aggregates of predetermined sizes are successfully prepared in the single stranded DNA: dye molecules are orderly aligned almost parallel to each other along the vertical axis of dye plane (see Scheme 2A).[2] To form H* aggregates of dyes, sequential multiplication of dyes is essential. Accordingly, insertion of spacer (**S** residue) between **D** residues interferes with H* aggregation (Figure 4). Promotion of H* aggregation by the presence of sufficient salt at low temperature demonstrates that hydrophobic stacking interaction between the adjacent dyes is the main driving force for aggregation. The stacked structure of Methyl Reds is also confirmed by the large hypochromic effect as usually observed for natural DNA hybridization: the molar extinction coefficient of Methyl Red in **D5** or **D6** at $\lambda_{max}$ is smaller than that in **D1**, as shown in Figure 1B despite the much smaller half-line-width of **D5** or **D6**.

Since Methyl Red moieties are tethered on chiral and optically pure D-threoninols, distinct CD are observed for all the **D*n*** around the absorption maximum. As expected, the CD spectrum

(18) A natural portion of oligonucleotides in the **D5/S*n*** duplex forms a right-handed B-type helix, since the symmetrical positive Cotton effect is observed around 260 nm. See Supporting Information Figure 5.

***Scheme 2.*** Proposed Aggregated Structures of Methyl Reds in the Single Stranded **D5** (A), by Hybridization with **S0** or **S1** (B), and by Hybridization with **S5** or **S6** (C)

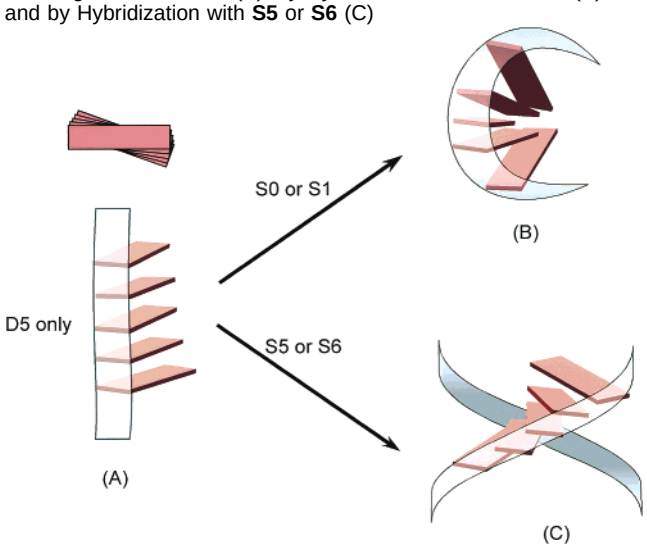


of opposite phase to **D6** is obtained for **L6** on L-threoninols (see Supporting Information Figure 6), indicating that the chirality of the linker determines the helicity. The CD signals at the $\pi-\pi^*$ transition of chromophores reflect the mutual orientation of the stacked dyes.[15,16] The positive Cotton effect observed for **D2** to **D6** indicate that Methyl Reds are stacked by forming right-handed helical structure as schematically illustrated in Scheme 2A.[16] But the winding of the helix should be small because the H* band is derived from the strong exciton coupling due to a large overlap of stacked dyes.[2] Otherwise the H* band should not appear (or the hypsochromic shift should be much smaller) because large winding makes the overlapped area of the stacked dyes small, which diminishes exciton coupling.

**Change of Aggregated Structure by Hybridization.** Addition of complementary DNA to **D6** or **D5** induces significant bathochromic shift of the H* band and change of the CD spectrum,[19] and the number of **S** residues in the complementary strand strongly affects spectroscopic behaviors. These facts demonstrate that the aggregated structure of dyes is controllable by its counterpart. Spectroscopic changes reflect the aggregated structures by hybridization. On the basis of both UV−vis and CD spectra, the following aggregation modes are deduced.

**(a) D5/S0 or D5/S1 Duplex.** With **S0** involving no **S** residue, $\lambda_{max}$ appears at 439 nm. Bathochromic shift with respect to the **D5** is 21 nm, which is smaller than that of the **D5/S5** or **D5/S6** duplex. This smaller bathochromic shift indicates that aggregated Methyl Reds maintain still strong exciton coupling among the dyes. In other words, the dyes in the **D5/S0** are still largely overlapped. Broad UV−vis spectra (half-line-width is 5142 cm$^{-1}$) with small absorbance and diminished CD signal reflect the disarranged structure. The same is also true for the **D5/S1** duplex. Thus, bulgelike arrangement of Methyl Reds is forced to be formed in the duplex, where dyes are stacked but in a disarranged manner as illustrated in Scheme 2B.

(19) Similarly, the spectral change of the aggregated Methyl Reds in **L6** is also observed on hybridization with **S6**: But in contrast with the **D6/S6** duplex, the CD spectrum of **L6/S6** at 0 °C did not exhibit a symmetrical Cotton effect and its intensity at 0 °C was weaker than that at 40 °C, probably reflecting partially left-handed arrangement of Methyl Reds in **L6** in the duplex: see Supporting Information Figure 7.

**(b) D5/S5 or D5/S6 Duplex.** When the number of **S** residues increases, the $\lambda_{max}$ monotonically shifts toward longer wavelength accompanied by narrowing of the band (see Table 1), and the magnitude of CD signal is again intensified (Figure 10B). On hybridization with **S5**, $\lambda_{max}$ appears at 452 nm and the bathochromic shift is as large as 34 nm, indicating that the overlapped area of mutual dyes should be smaller than the **D5/S0** or **D5/S1** duplex. A similar large bathochromic shift is also observed for the **D5/S6** duplex. Intensified positive Cotton effect demonstrates a right-handed helical structure. Thus, Methyl Reds form ordered a right-handed helix in the duplex, as illustrated in Scheme 2C. A sufficient number of **S** residues in the complementary strand slides closely stacked Methyl Reds by forming the helix. An increase in the absorbance by hybridization with **S5** or **S6** also indicates that closely stacked dyes (origin of hypochromicity for **D5**) are stretched. Consistently, $T_m$s of **D5/S5** and **D5/S6** are much lower than **D5/S0** and **D5/S1** (see Table 1), because hybridization with **S5** or **S6** loses more stacking interaction among the dyes than with **S0** or **S1**.

## Conclusions

(1) A novel Methyl Red H* aggregate of predetermined size is successfully prepared by multiplying dye residues in the single stranded DNA. The obtained Methyl Reds H* aggregate is sufficiently stable under high ionic strength.

(2) The Methyl Red H* aggregate in the single strand is converted into another aggregated structure by hybridization with the complementary strand, and its aggregated structure is controllable by the kinds of DNAs used for hybridization.

By programming the sequence of dyes and natural bases, various aggregates can be synthesized.

## Experimental Section

**Materials.** All the conventional phosphoramidite monomers, CPG columns, the reagents for DNA synthesis, and Poly-Pak cartridges were purchased from GLEN RESEARCH Co. Other reagents for the synthesis of phosphoramidite monomer were purchased from Tokyo Kasei Co. Ltd. and Aldrich.

**Synthesis of the Phosphoramidite Monomer.** The phosphoramidite monomer carrying a Methyl Red was synthesized as follows: D- or L-threoninol was obtained by the reduction of the corresponding D- or L-threonine methyl ester with $LiAlH_4$ in dry tetrahydrofuran (THF) according to the literature.[20] Then the D-threoninol (0.53 g, 5.0 mmol) was coupled with Methyl Red (4-[4-(dimethylamino)phenylazo]benzoic acid, 2.96 g, 10 mmol) in the presence of dicyclohexylcarbodiimide (DCC, 2.1 g, 10 mmol) and 1-hydroxybenzotriazole (HOBt, 1.35 g, 10 mmol) in 50 mL of dimethylformamide (DMF). After the reaction mixture was stirred at room temperature for 24 h, the solid part of the reaction mixture was removed by filtration. The filtrate was evaporated, and the obtained solid was subjected to recrystallization from $CHCl_3$:DMF = 5:1 mixed solvent (yield 60%): $^1$H NMR for **1** [DMSO-$d_6$ (TMS), 500 MHz] $\delta$ = 8.01 (d, $^3J$(H,H) = 8.5 Hz, 2H, aromatic protons), 7.84−7.81 (m, 5H, aromatic protons and −N*H*CO−), 6.85 (d, $^3J$(H,H) = 9.0 Hz, 2H, aromatic protons), 4.64−4.59 (m, 2H, −C*H*$_2$−OH), 3.94−3.91 (m, 2H, HOCH$_2$C*H*(NHCO−)C*H*(CH$_3$)OH), 3.64−3.49 (m, 2H, *H*OCH$_2$− and −CH(CH$_3$)O*H*), 3.08 (s, 6H, −N(CH$_3$)$_2$), 1.08 (d, $^3J$(H,H) = 6.0 Hz, 3H, −CH(OH)C*H*$_3$). ESI-MS for **1**: obsd 378.93 (calcd. for [**1** + Na$^+$] 379.08).

For tritylation of **1**, 4,4′-dimethoxytrityl chloride (DMT-Cl, 1.1 g, 3.4 mmol) in $CH_2Cl_2$ (5 mL) was added to dry pyridine solution (20 mL) containing **1** (1.0 g, 2.8 mmol) and (dimethylamino)pyridine (DMAP, 0.02 g, 0.17 mmol) in an ice bath under nitrogen. After 24 h of vigorous stirring, the solvent was removed by evaporation, followed by silica gel column chromatography (hexane:AcOEt:Et$_3$N = 50:50:3, $R_f$ = 0.41 (yield 74%)): $^1$H NMR for **2** [$CDCl_3$ (TMS), 500 MHz] $\delta$ = 8.00−6.76 (m, 22H, aromatic protons of DMT, Methyl Red; and −N*H*CO−), 4.23 (m, 1H, −C*H*(OH)CH$_3$), 4.12 (m, 1H, −OCH$_2$C*H*-(NHCO−)−), 3.77 and 3.76 (s, 6H, −C$_6$H$_4$−OC*H*$_3$), 3.60 and 3.39 (dd, $^2J$(H,H) = 10.0 Hz, $^3J$(H,H) = 4.0 Hz, 2H, −C*H*$_2$−ODMT), 3.11 (s, 6H, −N(CH$_3$)$_2$), 1.23 (d, $^3J$(H,H) = 6.5 Hz, 3H, −CH(OH)C*H*$_3$). ESI-MS for **2**: obsd 680.87 (calcd for [**2** + Na$^+$] 681.31).

In dry acetonitrile (10 mL) under nitrogen, **2** (0.158 g, 0.24 mmol) and 2-cyanoethyl *N*,*N*,*N*′,*N*′-tetraisopropylphosphorodiamidite (0.082 g, 0.27 mmol) were reacted with 1*H*-tetrazole (0.021 g, 0.30 mmol). Prior to the reaction, **2** and 1*H*-tetrazole were dried by coevaporation with dry acetonitrile (twice). After 2 h, the product was taken into 100 mL of ethyl acetate. The organic solution was washed with 100 mL of saturated aqueous solutions of $NaHCO_3$ and of NaCl and dried over $Na_2SO_4$. Finally the solvent was removed in vacuo, and the oily product **3** was directly used for the DNA synthesis.

**Synthesis of the Modified DNA Involving Methyl Red.** All the modified DNAs were synthesized on an automated DNA synthesizer by using **3**, the phosphoramidite monomer for **S** residue (from GLEN RESEARCH), and other conventional ones. The coupling efficiency of monomer **3** was as high as the conventional ones as judged from the coloration of released trityl cation. After the recommended workup, they were purified by the reversed-phase HPLC.[21]

MALDI-TOFMS. For **D1**: obsd 4058 (calcd for [**D1**−H$^+$] 4060). For **D2**: obsd 4478 (calcd for [**D2**−H$^+$] 4478). For **D3**: obsd 4895 (calcd for [**D3**−H$^+$] 4896). For **D4**: obsd 5317 (calcd for [**D4**−H$^+$] 5314). For **D5**: obsd 5733 (calcd for [**D5**−H$^+$] 5732). For **D6**: obsd. 6153 (calcd for [**D6**−H$^+$] 6151). For **L1**: obsd 4062 (calcd for [**L1**−H$^+$] 4060). For **L2**: obsd 4475 (calcd for [**L2**−H$^+$] 4478). For **L6**: obsd 6153 (calcd for [**L6**−H$^+$] 6151). For **DS4**: obsd 5868 (calcd for [**DS4**−H$^+$] 5866). For **S1**: obsd 3781 (calcd for [**S1**−H$^+$] 3780). For **S2**: obsd 3917 (calcd for [**S2**−H$^+$] 3918). For **S3**: obsd 4056 (calcd for [**S3**−H$^+$] 4056). For **S4**: obsd 4197 (calcd for [**S4**−H$^+$] 4194). For **S5**: obsd 4335 (calcd for [**S5**−H$^+$] 4332). For **S6**: obsd 4471 (calcd for [**S6**−H$^+$] 4470).

**Spectroscopic Measurements.** TheUV−visible and CD spectra were measured on a JASCO model V-530 and a JASCO model J-725, respectively, with a 10 mm (for UV measurement) or 1 mm (for CD measurement) quartz cell. Both of them were equipped with programmed temperature controllers. Conditions of the sample solutions were as follows (unless otherwise noted): [NaCl] = 0.1 M, pH 7.0 (10 mM phosphate buffer), [**Dn**] = [**Ln**] = 5 $\mu$M, [**Sn**] = [**C1**] = [**C2**] = 6 $\mu$M. The **Dn**:**Sn** and **D6**:**C1** (**C2**) ratios were kept 1:1.2 in order to secure that there exists no free **Dn**, which should disturb the UV and CD spectra.

**Measurement of Melting Temperature.** The melting curve of the duplex was obtained with rhw above apparatus by measuring the change of absorbance at 260 nm versus temperature. The melting temperature ($T_m$) was determined from the maximum in the first derivative of the melting curve. Both of the heating and cooling curves were measured, and the $T_m$ obtained from them coincided with each other within 2.0 °C. The $T_m$ values presented here are an average of two to four independent experiments. The error of $T_m$ values is ±1.0 °C.

**Acknowledgment.** This work was partially supported by a Grant-in-Aid for Scientific Research from the Ministry of Education, Culture, Sports, Science and Technology, Japan.

**Supporting Information Available:** Figures showing the schematic representation of the electronic transitions, the UV−

(20) Stanfield, C. F.; Parker, J. E.; Kanellis, P. *J. Org. Chem.* **1981**, *46*, 4799−4800.

(21) Asanuma, H.; Yoshida, T.; Ito, T.; Komiyama, M. *Tetrahedron Lett.* **1999**, *40*, 7995−7998.

vis spectrum of Methyl Red, the CD spectra of single stranded **D4** at various temperatures, the melting curves for **D5/S*n*** and **D*m*/S2** series, the CD spectrum of the **D5/S6** duplex (from 230 to 300 nm), the CD spectra of single stranded **D6** and **L6**, and the temperature dependence of UV−vis and CD spectra of the **L6/S6** duplex at various temperatures. This material is available free of charge via the Internet at http://pubs.acs.org.

JA021153K